RAPID COMMUNICATION

# Thermoplasmonics-assisted nanoheterostructured Au-decorated CuInS$_2$ nanoparticles: Matching solar spectrum absorption and its application on selective distillation of non-polar solvent systems by thermal solar energy

**Yu-Ting Yen[a], Chia-Wei Chen[a], Ming Fang[b], Yu-Ze Chen[a], Chih-Chung Lai[a], Cheng-Hung Hsu[a], Yi-Chung Wang[a], Hao Lin[b], Chang-Hong Shen[c], Jia-Min Shieh[c], Johnny C. Ho[b,*], Yu-Lun Chueh[a,*]**

[a]Department of Materials Science and Engineering, National Tsing Hua University, 30013 Taiwan, ROC
[b]Department of Physics and Materials Science, City University of Hong Kong, 83 Tat Chee Avenue, Kowloon, Hong Kong
[c]National Nano Device Laboratories, No.26, Prosperity Road 1, Hsinchu 30078, Taiwan

**Abstract**
In this work, enhanced broadband solar spectrum absorption and solar-thermal conversion efficiency (~ 8%) has realized and reported by Au-decorated CuInS$_2$ nanoparticles, namely Au@CIS NPs. The morphologies, compositions and absorptions were characterized by high resolution transmission electron microscopy (HR-TEM), UV-vis spectrometer and Finite-Difference Time-Domain (FDTD) numeric methods. The Au@CIS NPs shows a distinguished absorption perfectly matching AM1.5 G solar spectrum, compared with pure Au, CIS and CIS-Au mixture nanoparticles (NPs) owing to near field plasmonic-assisted effect. In addition, the Au@CIS NPs proves its practical applications on selective distillation in non-polar solvent systems, for which the selective distillation of methylcyclohexane from toluene as an example was demonstrated. The approach

---

*Corresponding authors.
*E-mail addresses:* johnnyho@cityu.edu.hk (J.C. Ho),
ylchueh@mx.nthu.edu.tw (Y.-L. Chueh).

can evoke future developments of plasmonic-assisted heterostructure in nanoscale for thermal solar energy harvesting application.

## Introduction

Nobel nanoparticles (NPs) are featured with its remarkable optical properties over the last decade, especially for the capability to serve as an excellent heat receiver irradiated under a wavelength of light corresponding to its plasmon resonance wavelength, which is called thermoplasmonics [1,2]. The thermoplasmonics effect can be collectively oscillated as set of resonances known as surface plasmon where the surface charges of metal nanostructures are triggered by electromagnetic waves [3]. The plasmon resonance appeared in a localized area at the interface between two materials are known as localized surface plasmon resonances (LSPR). Several metals, particularly gold (Au), silver (Ag) and cooper (Cu), which have metal conduction electrons, can coherently trigger the LSPR as a collective. The NPs heating source in nanoscale has been feasible at various applications such as nanothermal therapies [4], drug delivery system, [5] photoacoustic imaging, [6] nanochemistry [7] and plasmonic fluids, [8] opening up broad disciplines.

However, the intrinsic narrow window of plasmon resonance wavelength from these metal NPs limits its practical applications. To tackle and broaden absorption ranges of NPs, hybrid NPs such as $Fe_3O_4$/Au, [9] $SiO_2$/$Fe_2O_3$–Au, [10] Au/$TiO_2$, [11] Au/Pd, [12] $SiO_2$/Au, [13-16] Graphene/Au, [17] Ag/Au, [18] $SiO_2$/Ag [19] and $VO_2$/Au [20] have been proposed, which provide advantages of equivalent light absorption by an increase of absorption cross-section compared with the counterpart materials NPs, thereby consuming less volume of metal NPs. In addition, superimposing functionalities such as magnetic and optical dual properties can be contributed from hybrid NPs for possible applications at bio-imaging, [9] thermal ablation of bacterium [9] and ambient oxygen-free dehydrogenation of aromatic alcohols by catalytic-thermal plasmonic effect [12]. In order to efficiently harvest thermal solar energy, pursuing broadband absorption materials to match solar spectrum is imperative, which has been applied in the organic photovoltaics [21-23].

Copper indium disulfide (CIS) has been found as an excellent material to significantly harvest solar energy due to its direct bandgap, which fits well with the solar spectrum and high photostability characteristics [24,25]. Its high optical absorption coefficient ($10^4$ cm$^{-1}$ @ 750 nm) has been demonstrated a great potential as solar harvester. By combing the CIS with other functional nanomaterials, a beneficial effect serving the CIS as an efficient sensitizer to accompany functional materials in order to promote system performance has been demonstrated [26,27] However, no light-to-heat demonstration under the practical broadband solar spectrum was found by using $CuInS_2$ as sensitizer or illuminated under a narrow spectrum such as laser, restricting the possible applications to other fields. In this regard, we develop an ultimate high-absorption material $CuInS_2$ NPs decorated by gold NPs (Au@CIS NPs), exhibiting a broaden band perfectly matching the solar absorption spectrum for the light-to-heat conversion application. The findings indicate that Au NPs was deliberately anchored on the $CuInS_2$, exhibiting the enhanced plasmonic effect compared with randomly dispersive of the plasmonic Au NPs. Furthermore, solar-thermal conversion efficiency for Au@CIS, Au and CIS-Au mixture NPs were measured. The morphologies, compositions and absorptions were characterized by series of consistent results from HR-TEM, UV–vis spectrometer and FDTD numeric methods. Furthermore, the Au@CIS NPs prove its interesting application on selective distillation in non-polar solvent systems by harvesting thermal solar energy.

## Material and methods

### Synthesis of Au nanoparticles

20 mM of Gold(I) chloride (AuCl 99.9%) and 0.4 M of Oleylamine (70%) were mixed into a round flask with chloroform as solvent. After stirring for 3 min, the solution change its color from yellow to orange-red. Subsequently, the solution was heated to 60 °C by oil bath with continuous stirring and then hold for 6 h. Once upon completion of reaction, the Au nanocrystals were extracted by adding acetone (5 mL) followed by centrifuge at 10,000 rpm for 10 min. The precipitate was collected and repeated another extraction cycle by re-disperse precipitate with methanol (1 mL) and hexane (0.5 mL). Final precipitates were collected and re-dispersed in toluene for further analysis and experiments.

### Synthesis of $CuInS_2$ nanoparticles

$CuInS_2$ (CIS) nanocrystals (precursor) were synthesized by vacuum-free chemical method. 12 mL Oleylamine (70%), 0.5 mmol Copper(I) chloride (CuCl 99.995%), 0.5 mmol Indium (III) chloride (InCl$_3$, 99.999% anhydrous) and 1.0 mmol elemental sulfur powder (S, 99.998%) were mixed into a tri-neck beaker in a glove box and then attached to the heating mantle. The beaker temperature was slowly raised to 130 °C with a ramp of 2.3 °C/min for 1 h. Subsequently, the temperature was allowed to increase to 220 °C with an identical slope of previous stage and held at 220 °C for 1.5 h under vigorous stirring and argon gas. The beaker was then cooled down to room temperature (27 °C) by immersing beaker into a cold water bath. The CIS nanocrystals were extracted by a centrifugation process at 8000 rpm for 10 min by addition of 15 mL ethanol and 10 mL hexane. After repeating two cycles of centrifugation step, CIS NPs were precipitated and collected while the supernatant was discarded. The extracted CIS NPs were re-dispersed in toluene or stored in ambient condition for further applications.

## Synthesis of hybrid Au-decorated CuInS$_2$ nanoparticles

Au-decorated CuInS$_2$ NPs was synthesis by serving as synthesized CIS$_2$ NPs as seed. Seed solution was prepared by introducing CIS$_2$ NPs (946 ppm) into 30 mL of chloroform, and then allowed to raise temperature to 60 °C at the increasing rate of 5 °C/min for reflux under vigorous stirring and held for 10 min. Subsequently, 11.4 mL solution composed of 109 μmol gold(III) chloride trihydrate (HAuCl$_4$ · 3H$_2$O, 99.99%), 3 mL oleylamine (70%) and 8.4 mL chloroform were injected into the seed solution. Note that the solution changes its color from light yellow to orange-red when introducing oleylamine into gold(III) chloride trihydrate, indicating the formation of AuNPs. The entire system was hold at 60 °C for 5 h before cooling down to room temperature. The reaction solution was then purified by adding of excess ethanol and is subjected to centrifuge at 6000 rpm for 5 min to form the precipitate. After repeating two more cycle of purification step, the precipitate was collected as Au-decorated CuInS$_2$ NPs, which can be dispersed in most of nonpolar solvents such as chloroform, toluene and hexane. Note that separation of Au@CIS NPs from unreacted Au NPs can be achieved by adding over amount of Au precursor to guarantee the complete reaction of the CIS into Au@CIS NPs at the preparation step. The unreacted Au NPs can simply purified by centrifugation step due to the significant mass differences between AuNPs and Au@CIS NPs.

## Thermal energy generation by hybrid CuInS$_2$ NPs systems

Thermal energy generation was conducted by focused sunlight (a 260 mm × 260 mm Fresnel lens with focal length of 200 mm) or laser beam illuminated onto a 25 mL double neck flask with immersed thermal couple for real time temperature monitoring. The hybrid CuInS$_2$ NPs were composed of 7.5 mL Au@CIS NPs (500 ppm) dispersed in the toluene and the temperature were taken every 10 s until the boiling point of the toluene is reached. The conversion efficiencies estimation was taken by calculating the amount of energy required for elevated system temperature divided by total irradiance of solar energy within 30 s (i.e. (thermal energy required for elevated system temperature/solar irradiance) × 100%). Note that we ignore any loss or absorption of heat from the imperfect system by simply assuming that all of solar energy focused by Fresnel lens will be absorbed by the whole system.

## Numerical (FDTD simulation)

The finite-difference time-domain (FDTD) simulation was conducted via FDTD Solutions 8.0 software. A 80 × 80 nm$^2$ region with 1 nm meshes in general and 0.1 nm fine meshes were used to overlap on the Au nanoparticles and plane waves were used as the source for the calculation and illuminated from the left. Refractive index of AuNPs were taken from "Au (Gold)-CRC" default material database and that of CuInS$_2$ was referred from the report by Alonso et al. [28].

## Measurements and characterization

Morphologies, lattice spacing and elemental compositions were acquired by high resolution transmission electron microscopy (HRTEM, JEOL, JEM-3000F FEGTEM, 300 kV) equipped with Energy Dispersive Spectroscopy (EDS by INCA analysis system, Oxford Instruments). Absorption spectroscopy was acquired by spectrophotometer (Hitachi, U-4100 UV-visible-NIR Spectrophotometer), with concentrations of 0.29 g L$^{-1}$ and 0.51 g L$^{-1}$ for CuInS$_2$ and Au NPs dispersed in toluene, respectively. The concentration for CIS-Au mixture has identical contents, corresponding to the pure NPs samples (i.e. 0.29 g L$^{-1}$ of CuInS$_2$ and 0.51 g L$^{-1}$of Au NPs in the mixture). In order to compare the absorption results of Au decorated CIS NPs with the mixture, the absorbance of Au decorated CIS NPs was set equivalent to the mixture at wavelength of 330 nm. Laser was spotted by a diode laser with the wavelength and power of 808 nm and 30 W, respectively. Solar irradiation was conducted under a standard AM 1.5 G solar simulator (Class AAA Solar Simulator, Newport) with intensity of 1000 W/m$^2$.

## Results and discussion

Figure 1a-c shows typical TEM images of CuInS$_2$, Au and Au@CIS NPs. Insets show the corresponding HR-TEM images, with which the corresponding average diameters were listed in Figure S1. Obviously, the diameters of ∼25 and ∼4 nm in average for CIS and Au NPs can be measured. For the Au@CIS NPs, Au NPs with the average diameter of ∼4 nm are uniformly decorated on the entire surface of CIS NPs. All NPs diameter in this work were designed to be less than
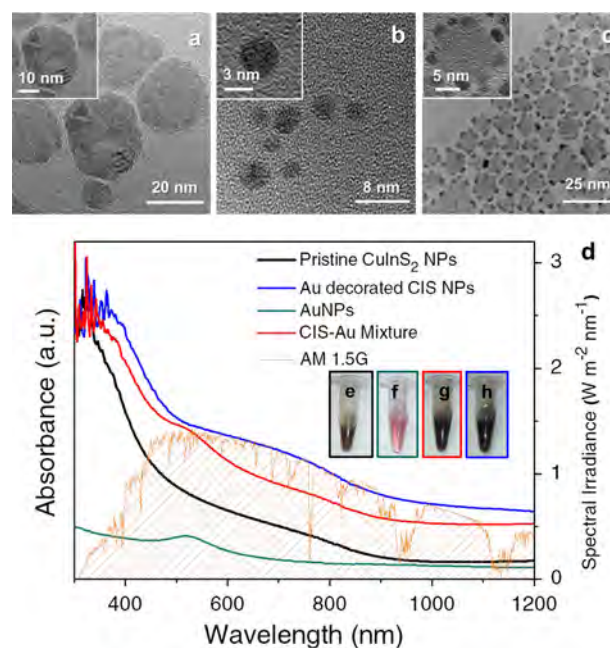


**Fig. 1** TEM images and absorption spectra of CuInS$_2$, Au and Au decorated CuInS$_2$ NPs. (a) CuInS$_2$, (b) Au, (c) Au decorated CuInS$_2$ NPs, and (d) the corresponding, absorption spectra Optical images of (e) CIS, (f) Au, (g) mixture of CIS with Au and (h) Au decorated CIS NPs, respectively. Yellow curve in insets shows an AM 1.5 G solar spectra as the reference.

50 nm, which is dedicated to convert thermal energy by absorption of incident light [13]. Compositions of Au@CIS NPs being 7.1%, 18.7%, 18.1% and 56.1% for Cu, Au, In and S elements measured from the selected area by the energy dispersive spectrometer (EDS) were listed in Table S1, respectively (Figure S2a). Note that the stoichiometry of Au@CIS NPs are similar to the regular CuInS$_2$, for which the stoichiometry ratio was found to be 1:1:2 for Cu, In and S, respectively, indicating an evidence that Au atoms substitutionally replace Cu atoms during the synthesis procedure. Furthermore, lattice spacings of 0.396 and 0.237 nm revealed by high resolution TEM images are consistent with (110) and (111) planes of CIS and Au, respectively (Figure S2b). In addition, the Au@CIS NPs can be easily purified from other unreacted CIS or Au NPs by simple centrifuge process. (For detailed process please refer to *Materials and Method* section). Moreover, we found that the compact Au@CIS NPs exhibits the better stability than CIS-Au mixtures due to the solution system containing single phase rather than dual phases. Figure 1d shows absorbance spectra for CIS, Au, CIS-Au mixture and Au@CIS NPs, respectively, with which the concentration of 0.29 g L$^{-1}$ and 0.51 g L$^{-1}$ for the CIS and the Au were dispersed in toluene and the CIS-Au mixture has identical concentration with individual pure NPs (i.e. 0.29 g L$^{-1}$ of CIS and 0.51 g L$^{-1}$ of Au NPs in the mixture). In order to compare the absorption enhancement between the CIS-Au mixture and the Au@CIS NPs, the Au@CIS NPs concentrations were equivalently set to absorbance intensity of the CIS-Au mixture NPs at the wavelength of 330 nm, the highest

intensify peak of the CIS-Au mixture. Obviously, the corresponding regular broad plasmon resonance peak at ~525 nm attributed to Au NPs can be measured, which agrees with the literature report (Green curve in Figure 1d). [29] For CIS NPs, the board band absorption ranging from 400 to 800 nm can be measured and for CIS-Au mixture, minor enhancement from the plasmon resonance characteristic peak at visible light ranges can be achieved, which is superimposed by resonance characteristic peaks of Au and CIS together (Red curve in Figure 1d). On the contrary, for Au@CIS NPs, an obvious broadband absorption perfectly matching the solar spectrum (yellow curve in Figure 1d) can be found (Blue curve in Figure 1d).

To prove the enhanced absorption mechanism achieved by Au@CIS NPs compared with other hybrid NPs, 2D Finite-Difference Time-Domain (FDTD) simulation was conducted to predict the ideal absorbance spectra as the function of the solar wavelengths from 300 to 800 nm as shown in Figure 2a and b. Since visible light covers most of solar spectrum, intensity should be counted for evaluation of harvesting solar irradiation. Note that for both pristine CIS and Au NPs, the absorption shows single wave pattern. However, CIS-Au mixture and Au@CIS NPs present multiple absorption behaviors. Especially, for Au@CIS NPs, broaden and plateau-like absorption spectra proves the enhanced absorption at visible solar wavelengths around 550-800 nm, which can be observed by the calculated enhancement factor. To shed light on enhanced absorption by the Au@CIS NPs, the enhancement factor ($F_{Abs}$) defined by the absorbance ratio of the Au@CIS NPs to the CIS-Au mixture (i.e. Abs$_{Au@CIS}$/Abs$_{CIS-Au\ mixture}$) was
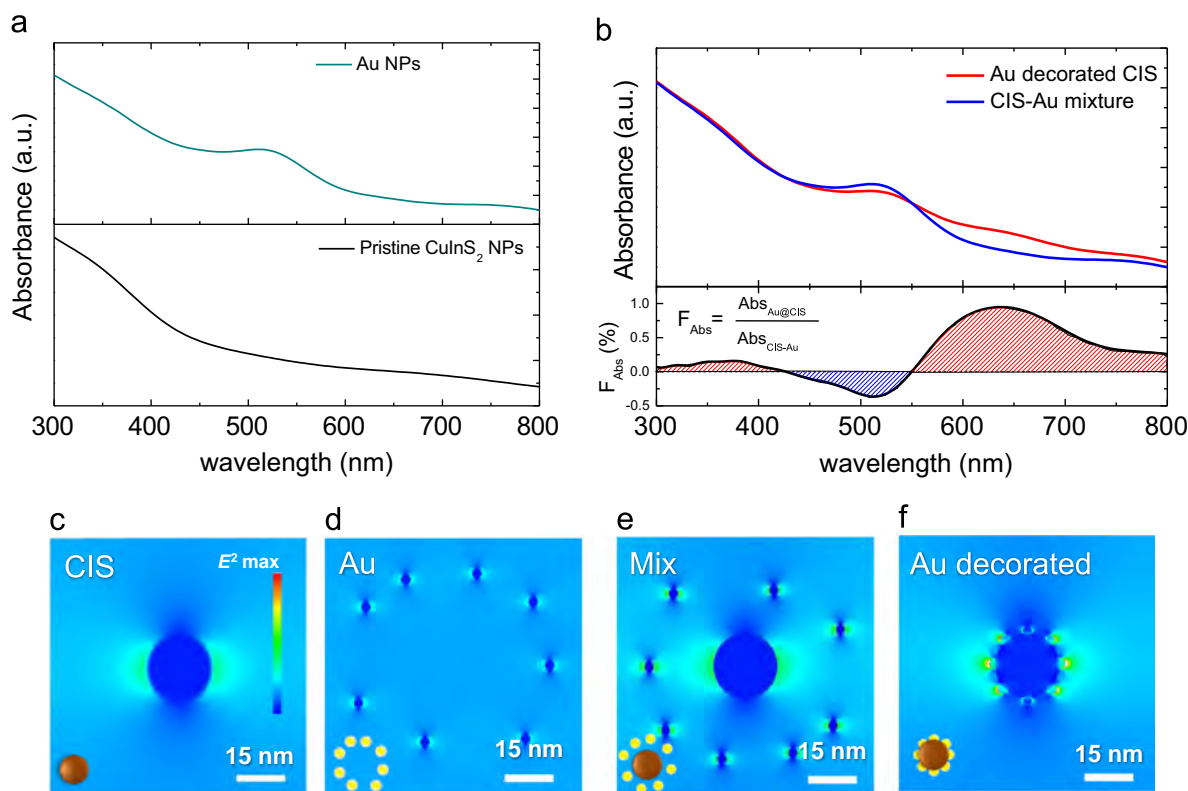


**Fig. 2** FDTD simulated results. (a) plot of simulated absorption spectra for pristine CIS, Au and (b) Mixture of CuInS$_2$ with Au, Au decorated CuInS$_2$ NPs and enhancement factor of Au decorated CuInS$_2$ to mixture as function of wavelength. 2D electrical field mapping results on (c) CIS, (d) Au, (e) mixture of CuInS$_2$ with Au and (f) Au decorated CuInS$_2$ NPs, respectively.

plotted as the function of wavelengths in Figure 2b. Further-more, we further choose 2D electromagnetic(EM) field($|E|^2$) spatial distribution at 800 nm for CIS, Au, CIS–Au mixture and Au@CIS NPs in the toluene as medium as shown in Figure 2c–f, respectively. Both materials were further fitted into multi-coefficient models, with which the dielectric constant of toluene (1.497) was used as the background. To avoid boundary absorption effect, periodic boundaries were employed for the y dimension and perfectly matched layer (PML) for the x dimension. Obviously, the EM response under the visible light clearly shows the surrounding strong local-ized field for Au@CIS NPs. Intensity of these "hot spots" for Au@CIS NPs is significantly stronger than that of CIS, Au and CIS–Au mixture NPs. The results indicate that the calculated absorbance spectra match well with the experiments results. Especially, as the loading ratios by surface area of Au to CIS NPs increase from 6.4% to 50.9%, the absorption capability at visible region evidently become broader (Figure S3) while no broaden absorption but only characteristic of plasmon reso-nance peak was observed by simply mixing of Au and $CIS_2$ NPs (Figures S4 and S5 ). The broadband enhancement of the light absorption in the Au@CIS NPs could be contributed by induced charge transfer and the higher refractive indices than its surrounding toluene medium because of the over-lapping of electronic states from hybrid nanocomponents of metal-semiconductors [30,31]. It has reported that the red-shift of plasmon peak can be observed by electron deficiency hybridization of Au–$Fe_3O_4$ dumbbell structures due to charge variation [32] and more significant shift of peak can be also observed on hybridization of high refractive index $Fe_3O_4$ domain with Au [33]. Shape/size variation of metal nano-particles could also be a possible factor, leading to shift of resonation peaks [34]. However, in our case, the limited changes on Au particles size would not result in such large peak shift to the broadband absorption enhancement from the 600 to 800 nm. Therefore, we believe that the broadband absorption of the Au@CIS NPs is most likely the charge transfer between Au and CIS owing to the hybridization of electron deficiency of Au combined with high refractive index of CIS ($\sim$2.7) [35]. This is why the broaden absorption spectrum created by Au@CIS NPs cannot be reproduced by simple mixture of linear combination with CIS and Au NPs.

Photothermal effect, namely thermal energy generation, triggered by plasmon resonance using colloidal NPs has been attracted much attention when the electromagnetic wave frequency coherently meets with the collective resonance of colloidal NPs. The mechanism of thermal energy genera-tion can be due to strong interaction between electromag-netic wave and mobile carriers inside the NPs, resulting in energy gained by thermal heating effect via phonon scatting between electrons and NPs. Subsequently, thermal energy diffuses away from the NPs to surrounding medium, leading to the elevated temperature in the whole system. Note that the heating effect is especially stronger for metal NPs in the regime of plasmon resonance because of many mobile electrons. Thus, the total amount of the thermal energy can be estimated in a relatively simple way as the total optical absorption rate due to a very low optical quantum yield [36,37]. These statements were evidenced by thermal heating experiments for well-dispersed Au, CIS, CIS–Au mixture and Au@CIS NPs in a typical nonpolar solvent such as toluene illuminated by an monochromatic light (laser

diode) with a wavelength of 808 nm as shown in Figure 3a, for which the pure toluene was used as a control reference and the corresponding experimental setup is shown in inset. Obviously, no elevated temperature can be found for the pure toluene and Au NPs in the toluene solvent due to intrinsic absence of absorption capability at the wavelength of 808 nm. However, distinct thermal heating effect can be found from heat dissipation by CIS NPs due to absorption of laser light through an interband absorption process by the creation of mobile electrons and holes (exciton) in CIS NPs, leading to the elevated temperature of the whole system reaching to $\sim$100 °C after the illuminating time of $\sim$500 s. After mixture of Au with CIS NPs (CIS–Au mixture case), the heat dissipation through CIS to the toluene solvent can be further enhanced by metallic Au NPs, resulting in the faster heating rate to reach $\sim$100 °C within $\sim$450 s. Interestingly,
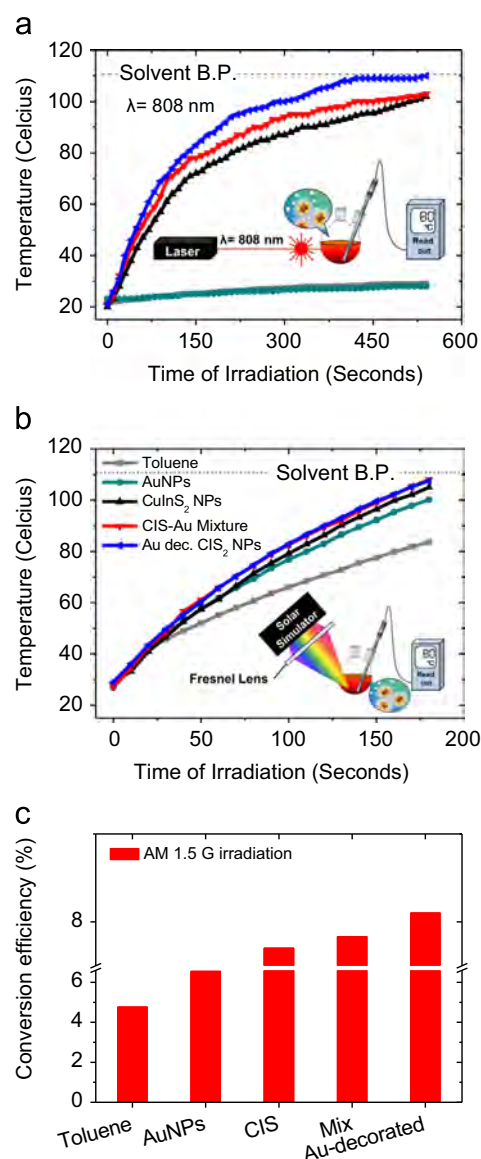


**Fig. 3** Thermal energy generation by hybrid $CuInS_2$ NPs systems. Temperature profiles for thermal energy generation by (a) laser and (b) AM 1.5 G solar spectrum. (c) conversion efficiencies under AM 1.5 G irradiation.

the distinctly enhanced light absorption at the wavelength of 808 nm for Au@CIS NPs case can be achieved with the temperature of the toluene solvent reaching to $\sim$110 °C (Solvent boiling point of toluene, B.P.) within $\sim$430 s. Furthermore, the feasibility of thermal heating experiments utilizing the solar energy for the non-polar solvent system was also performed under the solar irradiation with AM 1.5 G as shown in Figure 3b whose the experimental setup is shown in inset. Obviously, the thermal heating effect quickly responses to all samples at early stage within 30 s. However, differentiation of thermal heating rates can be distinctly observed with the thermal heating orders of Au@CIS$>$CIS–Au mixture$>$CIS$>$Au after the solar irradiation of 30 s. The remarkable result for reaching the boiling point of solvent is less than 200 s for Au@CIS NPs. We believe that the faster heating rate are attributed to the interplay between light scattering and the near-field plasmonic effect of anchored metallic Au on the CIS NPs surface, which triggers the near-field plasmonic effect by the fixed distance. In addition, the conversion efficiency was roughly evaluated as shown in Figure 3c with $\sim$8.1% for the Au@CIS NPs, $\sim$7.8% for CIS–Au mixture, $\sim$7.7% for CIS and $\sim$6.6% for Au NPs, respectively, by the thermal energy to the elevated temperature divided by the solar irradiation while ignoring any imperfect heat loss from apparatus or system (For details please refer to the *Materials and Method* section). We believe that the system performance can be improved with further development by minimizing heat loss and become more adaptable to the practical applications.

Owing to the localized hot spots surrounded to all well-dispersed Au@CIS NPs, which beneficially broaden the absorption spectra, leading to the locally generated thermal heating, Au@CIS NPs can further be utilized to select the favor solvent by anchoring the non-polar ligand on Au@CIS NPs. It gives Au@CIS NPs the potential to selectively heat the polarity solvent for separation application in similar solvents. To realize this concept, separation of methylcyclohexane (MCH) from toluene *via* selective heating process by Au@CIS NPs anchored by a non-polar oleylamine ligand under AM 1.5 G irradiation was demonstrated as shown in Figure 4 where the mole fractions of the MCH were measured in vapor and in liquid solutions from 0 to 1 with a step of 0.05, respectively. The generated vapor was directly
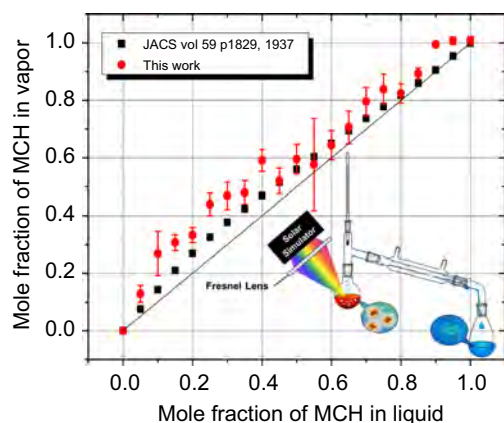
channeled into the condenser without experiencing any fractional column. Thermal heating source was applied by solar simulator with focusing Fresnel lens as the fluid heating step. Each mole fraction of MCH from the final distillate was identified by calibrating curves (Figure S6) after three independent replicates to avoid possible deviations of results. Note that the conventional separation of the MCH from the toluene by distillation approach was also plotted as reference in Figure 4 [38]. Obviously, after adding of Au@CIS NPs, the separation yield of the MCH is higher than that of the regular distillation process in the most of mole fraction cases. The enhanced selectivity can be attributed to the natural solvent polarity to the surrounded non-polar oleylamine ligand on Au@CIS NPs, for which polarity can be referred to the normalized empirical parameter ($E_T^N$) [39] as the polarity magnitude is in the decreasing order of toluene and cyclohexane (i.e. cyclohexane is less polar than toluene). The oleylamine ligand on the Au@CIS NPs can be decomposed into octadecene, which is a long-alkyl chain molecule with very low polarity [40]. It makes the MCH bonded with the Au@CIS NPs due the similar polarity rather than toluene by formation of dipole interactions. As a result, the MCH can receive much higher thermal energy than that of the toluene from the localized hot spots surrounding to the Au@CIS NPs, which explain the high mole faction in vapor, leading to the selective distillation. Moreover, the high surface area of nanoparticles also a benefit for the improved distillation yield [41]. On the other hand, the convection flow during the heating process occurs simultaneously, [1] which impede the NPs to adhere to the less polarity solvent from its full potential might deteriorate the distillation performance. We believe that the selective distillation by solar energy achieved by non-polar solvent systems can open up a possible opportunity to efficiently make distillation without electricity supply becoming possible in remote regions. The concept of the study can also be applied into non-polar solvent heating/distillation systems to reserve energy consumptions and provide opportunities toward developments of plasmonic-assisted heterostructure nanoparticles utilizing thermal solar energy. Further investigation toward solar energy harvesting such as water/molecular splitting, photocatalysis and sterilization by highly absorptive complex plasmonic-assisted nanoparticles can be highly expected.

## Conclusions

In summary, we have developed Au decorated CuInS$_2$ nanoparticles (Au@CIS NPs) for the light-to-heat conversion application with the ultimate high and broaden band solar absorption characters. The morphologies, compositions and absorption spectra of Au@CIS NPs were characterized by series of consistent results from HR-TEM, UV–vis spectrometer and FDTD numeric methods, respectively. Furthermore, enhanced broadband solar spectra and solar-thermal conversion efficiency reaching to $\sim$8.1% have been measured. In addition, selective distillation between methylcyclohexane from toluene by the Au@CIS NPs was demonstrated. In the future, imperfect light to heat conversion performance should emphasized more by the optimization of morphologies and distributed concentrations of hybrid heternanostructures to further tailor perfomance in a controllable manner. The



**Fig. 4** Distillation of methylcyclohexane with toluene utilize Au decorated CuInS$_2$ NPs. Inset shows the apparatus set up for distillation.

concept of the decorated NPs in this work can be applied into non-polar solvent heating/distillation systems and provides opportunities toward development of other metal nanodomain onto semiconductor nanocrystal to form versatile functional heternanostructures. Furthermore, investigation toward solar energy harvesting such as water/molecular splitting, photocatalysis and sterilization by highly absorptive complex plasmonic-assisted nanoparticles can be realized.

## Acknowledgments

## Appendix A.    Supporting information

Supplementary data associated with this article can be found in the online version at http://dx.doi.org/10.1016/j.nanoen.2015.04.031.

## References

[1] H.H. Richardson, M.T. Carlson, P.J. Tandler, P. Hernandez, A.O. Govorov, Nano Lett. 9 (2009) 1139-1146.
[2] G. Baffou, R. Quidant, Laser Photonics Rev. 7 (2013) 171-187.
[3] G. Baffou, R. Quidant, F.J. García de Abajo, ACS Nano 4 (2010) 709-716.
[4] L.C. Kennedy, L.R. Bickford, N.A. Lewinski, A.J. Coughlin, Y. Hu, E.S. Day, J.L. West, R.A. Drezek, Small 7 (2011) 169-183.
[5] J. Croissant, J.I. Zink, J. Am. Chem. Soc. 134 (2012) 7628-7631.
[6] K. Wilson, K. Homan, S. Emelianov, Nat. Commun. 3 (2012) 618.
[7] L. Cao, D.N. Barsic, A.R. Guichard, M.L. Brongersma, Nano Lett. 7 (2007) 3523-3527.
[8] K. Wang, E. Schonbrun, P. Steinvurzel, K.B. Crozier, Nat. Commun. 2 (2011) 469.
[9] C.G. Wang, J. Irudayaraj, Small 6 (2010) 283-289.
[10] M. Ramasamy, S.S. Lee, D.K. Yi, K. Kim, J. Mat. Chem. 2 (2014) 981-988B 2 (2014) 981-988.
[11] W. Chen, Y. Lu, W. Dong, Z. Chen, M. Shen, Mater. Res. Bull. 50 (2014) 31-35.
[12] S. Sarina, S. Bai, Y.M. Huang, C. Chen, J.F. Jia, E. Jaatinen, G.A. Ayoko, Z. Bao, H.Y. Zhu, Green Chem. 16 (2014) 331-341.
[13] W. Lv, P.E. Phelan, R. Swaminathan, T.P. Otanicar, R.A. Taylor, J. Sol. Energy Eng. Trans.-ASME 135 (2013) 021004.
[14] S. Mukherjee, L.A. Zhou, A.M. Goodman, N. Large, C. Ayala-Orozco, Y. Zhang, P. Nordlander, N.J. Halas, J. Am. Chem. Soc. 136 (2014) 64-67.
[15] N.J. Halas, O. Neumann, A. Urban, N. Hogan, Z.Y. Fang, A. Pimpinelli, S. Lal, P. Nordlander, Abstr. Pap. Am. Chem. Soc. 246 (2013).
[16] J.-J. Chen, J.C.S. Wu, P.C. Wu, D.P. Tsai, J. Phys. Chem. C 116 (2012) 26535-26542.
[17] S.R. Sahu, M.M. Devi, P. Mukherjee, P. Sen, K. Biswas, J. Nanomater. (2013) 232409.
[18] M.A. Uppal, M.B. Ewing, I.P. Parkin, Eur. J. Inorg. Chem. (2011) 4534-4544.
[19] J.H. Hsieh, C. Li, Y.Y. Wu, S.C. Jang, Thin Solid Films 519 (2011) 7124-7128.
[20] D.W. Ferrara, E.R. MacQuarrie, J. Nag, A.B. Kaye, R.F. Haglund, Appl. Phys. Lett. 98 (2011) 241112.
[21] Y.F. Li, Y.P. Zou, Adv. Mater. 20 (2008) 2952-2958.
[22] Y.Y. Liang, L.P. Yu, Acc. Chem. Res. 43 (2010) 1227-1236.
[23] W.Y. Wong, X.Z. Wang, Z. He, K.K. Chan, A.B. Djurisic, K.Y. Cheung, C.T. Yip, A.M.C. Ng, Y.Y. Xi, C.S.K. Mak, W.K. Chan, J. Am. Chem. Soc. 129 (2007) 14372-14380.
[24] S. Wagner, P.M. Bridenbaugh, J. Cryst. Growth 39 (1977) 151-159.
[25] J. Álvarez-García, A. Pérez-Rodríguez, A. Romano-Rodríguez, J.R. Morante, L. Calvo-Barrio, R. Scheer, R. Klenk, J. Vac. Sci. Technol. A 19 (2001) 232-239.
[26] K.-T. Kuo, D.-M. Liu, S.-Y. Chen, C.-C. Lin, J. Mater. Chem. 19 (2009) 6780-6788.
[27] T.-L. Li, H. Teng, J. Mater. Chem. 20 (2010) 3656-3664.
[28] M.I. Alonso, K. Wakita, J. Pascual, M. Garriga, N. Yamamoto, Phys. Rev. B 63 (2001) 075203.
[29] S.S. Kumar, C.S. Kumar, J. Mathiyarasu, K.L. Phani, Langmuir 23 (2007) 3401-3408.
[30] A.E. Saunders, I. Popov, U. Banin, J. Phys. Chem. B 110 (2006) 25421-25429.
[31] D. Steiner, T. Mokari, U. Banin, O. Millo, Phys. Rev. Lett. 95 (2005) 056805.
[32] H. Yu, M. Chen, P.M. Rice, S.X. Wang, R.L. White, S. Sun, Nano Lett. 5 (2005) 379-382.
[33] W. Shi, H. Zeng, Y. Sahoo, T.Y. Ohulchanskyy, Y. Ding, Z.L. Wang, M. Swihart, P.N. Prasad, Nano Lett. 6 (2006) 875-881.
[34] M. Hu, J. Chen, Z.-Y. Li, L. Au, G.V. Hartland, X. Li, M. Marquez, Y. Xia, Chem. Soc. Rev. 35 (2006) 1084-1094.
[35] M.I. Alonso, K. Wakita, J. Pascual, M. Garriga, N. Yamamoto, Phys Rev B 63 (2001) 075203.
[36] D. Lapotko, Opt. Exp. 17 (2009) 2538-2556.
[37] N. Harris, M.J. Ford, M.B. Cortie, J. Phys. Chem. B 110 (2006) 10701-10707.
[38] D. Quiggle, M.R. Fenske, J. Am. Chem. Soc. 59 (1937) 1829-1832.
[39] C. Reichardt, Solvents and Solvent Effects in Organic Chemistry, Wiley-VCH Verlag GmbH & Co. KGaA471-507 Printed in Federal Republic of Germany.
[40] S. Mourdikoudis, L.M. Liz-Marzán, Chem. Mater. 25 (2013) 1465-1476.
[41] O. Neumann, A.S. Urban, J. Day, S. Lal, P. Nordlander, N.J. Halas, ACS Nano 7 (2012) 42-49.

Yu-Ting Yen received his B.S. degree with high honors from Department of Biomedical Engineering & Environmental Sciences, National Tsing Hua University, Taiwan in 2010. Afterward, he pursued his Ph.D degree and became a Ph.D. candidate since 2012 at Department of Materials Science and Engineering, National Tsing Hua University, Taiwan. During his Ph.D. program he has earned several scholarships and international conference poster awards. His research interest focus on preparation of zero and one dimensional chalcopyrite nanostructures and their possible applications toward renewable energy and metrology. He will join Industrial Technology Research Institute (ITRI) in Taiwan after he receives his Ph.D. in July, 2015. Details can be found at: http://www.researchgate.net/profile/Yu-Ting_Yen

**Chia-Wei Chen** received her B.S. degree from National Tsing Hua University, Taiwan in 2011 and she commenced her Ph.D. program and became Ph.D. candidate in 2013 at Department of Materials Science and Engineering, National Tsing Hua University, Taiwan. Her research interests including interface passivation of thin film photovoltaics and synthesis of plasmonic nanocrystals.

**Ming Fang** received his B.S. and M.S. degrees from Huaqiao University, China and he is currently a Ph.D candidate at Department of Physics and Materials Science, City University of Hong Kong. His research interests focus on developing innovative techniques for nanostructure fabrications and exploring their possible applications in photovoltaics and artificial photosynthesis.

**Yu-Ze Chen** received his M.S. degree from Department of Materials Science and Engineering, National Tsing Hua University, Taiwan in 2010. He started his Ph.D. program and became Ph.D. candidate in 2012 at Department of Materials Science and Engineering, National Tsing Hua University, Taiwan. His research interests are developing low-temperature processes for preparing two-dimensional materials including graphene and two-dimensional transition metal dichalcogenides and its applications. From 2015, he joined Prof. Duan's group in UCLA Department Of Chemistry & Biochemistry, United State as a visiting researcher.
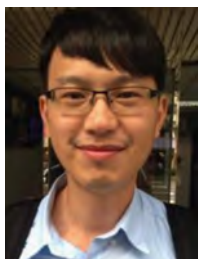
**Chih-Chung Lai** received his M.S. degree from institute of Materials Science and Engineering, National Central University, Taiwan in 2010. Now, he is a Ph.D. candidate at Department of Materials Science and Engineering, National Tsing Hua University. He research interests include: desalination techniques, 1D nano-structures fabrication, and synthesis of nanomaterials for renewable energy applications.

**Cheng-Hung Hsu** is pursuing his second year of M.S degree at Department of Materials Science and Engineering, National Tsing Hua University. He is also doing his research about CIGS solar cell in National Nano Device Laboratories (NDL), Taiwan.

**Yi-Chung Wang** received his B.S. degree in materials science and engineering from National Tsing Hua University (NTHU), Hsinchu, Taiwan in 1999, and now he is a Ph.D. candidate at Department of Materials Science And Engineering of NTHU.

**Hao Lin** received his M.S. degree from Institute of Optics and Optoelectronics, Faculty of Science, Ningbo University, China in 2013. Now, he is a Research Assistant at Department of Physics and Materials Science, City University of Hong Kong. His research interests include the fabrication and optical simulation of silicon based 3D nanostructures for photovoltaic applications.

**Chang-Hong Shen** received his Ph.D. in Physics at National Tsing-Hua University in 2006. From 2007, he joined MOSEL VITELIC INC in Taiwan. From 2009, he joined National Nano Device Laboratories as associate researcher. Currently he is a Research fellow and Division Director of advanced device division in NDL. His academic interests include photovoltaic devices, flexible electronics, and low-temperature laser/plasma processing. His current research focuses on developing low-cost, third-generation Si and CIGS thin-film solar cells, and low-temperature 3D nanoelectronics. Details can be found at: http://www.ndl.narl.org.tw/web/eng/research/ENERGY_-Manpower.php.

**Jia-Min Shieh** received his Ph.D. in Electro-Optics at National Chiao-Tung University, Taiwan in 1997. From 1998, he joined National Nano Device Laboratories (NDL), Taiwanandbecamearesearcherfrom2003. He leads the photovoltaic/photonic device division and Emerging Device Division in NDL from 2008 to 2013.Currently he is Deputy Director General in NDL. His academic interests include photovoltaic/photonic devices, flexible electronics, and low-temperature laser/plasma processing. His current research focuses on developing low-cost, nanoelectronics. Details can be found at: http://www.ndl.narl.org.tw/web/research/JMShieh.php.

**Johnny C. Ho** received his B.S. degree with high honors in Chemical Engineering, and M.S. and Ph.D. degrees in Materials Science and Engineering from the University of California, Berkeley, in 2002, 2005 and 2009, respectively. From 2009 to 2010, he worked in the nanoscale synthesis and characterization group at Lawrence Livermore National Laboratory, California. Currently, he is an Assistant Professor of Physics and Materials Science at the City University of Hong Kong. His research interests focus on the synthesis, characterization, integration and device applications of nanoscale materials for various technological applications, including nanoelectronics, sensors and energy harvesting. Details can be found at: http://www.ap.cityu.edu.hk/personal-website/johnny/site_flash/index.html.

**Yu-Lun Chueh** received his Ph.D degree from department of materials science and engineering, National Tsing Hua University, Taiwan in 2006 and worked as a post-doctoral research fellow in Electrical Engineering and Computer Science, UC Berkeley from 2007-2009. He joined Department of Materials Science and Engineering, National Tsing Hua university in 2009. Currently, He is associate professor in Department Of Materials Science

And Engineering, National Tsing Hua University, Taiwan. His research directions include (1) Development of Cu(In,Ga)Se$_2$ solar cell and its investigation on light harvesting behaviors, (2) Growth of low dimensional materials and its possible functional applications, (3) Low power resistive random access memory, (4) Development of various method to synthesize different Graphene/two dimensional materials and (5) Development of Electrically Charged-Induced Selective Ions in porous nanostructures and its application on Desalination of Saline Water. Details can be found at: http://nanoscienceandnanodevicelab.weebly.com/index.html.